IRIS RECOGNITION BASED ON FEATURE EXTRACTION

by

DEEPTHI RAMPALLY

B.Tech, Jawaharlal Nehru Technological University, India, 2007

A REPORT

submitted in partial fulfillment of the requirements for the degree

MASTER OF SCIENCE

Department of Electrical and Computer Engineering
College of Engineering

KANSAS STATE UNIVERSITY
Manhattan, Kansas

2010

Approved by:

Major Professor
Dr. D .V. Satish Chandra

Abstract

Biometric technologies are the foundation of personal identification systems. A biometric system recognizes an individual based on some characteristics or processes. Characteristics used for recognition include features measured from face, fingerprints, hand geometry, handwriting, iris, retina, vein, signature and voice. Among the various techniques, iris recognition is regarded as the most reliable and accurate biometric recognition system. However, the technology of iris coding is still at an early stage.

Iris recognition system consists of a segmentation system that localizes the iris region in an eye image and isolates eyelids, eyelashes. Segmentation is achieved using circular Hough transform for localizing the iris and pupil regions, linear Hough transform for localizing the eyelids and thresholding for detecting eyelashes. The segmented iris region is normalized to a rectangular block with fixed polar dimensions using Daugman's rubber sheet model. The work presented in this report involves extraction of iris templates using the algorithms developed by Daugman. Features are then extracted from these templates using wavelet transform to perform the recognition task. Method of extracting features using cumulative sums is also investigated. Iris codes are generated for each cell by computing cumulative sums which describe variations in the grey values of iris.

For determining the performance of the proposed iris recognition systems, CASIA database and UBRIS.v1 database of digitized grayscale eye images are used. K-nearest neighbor and Hamming distance classifiers are used to determine the similarity between the iris templates. The performance of the proposed methods is evaluated and compared.

Table of Contents

List of Figures

List of Tables

Acknowledgements

I thank my advisor, Dr. D.V.Satish Chandra for his support and guidance throughout the project. This project used the CASIA database collected by Chinese Academy of Sciences. I thank them for the eye images that were useful to this project. I also thank Libor Masek for using his segmentation and normalization algorithms mentioned in his thesis work for extracting the iris region from an eye image. I extend my gratitude to Dr. Don Gruenbacher and Dr. Chris L. Lewis for being my Committee members and reviewing this work.

I must also thank my parents Mr. Jagan Mohan and Mrs. Aruna Kumari, my husband Ramakrishna Nallamalli, for their love and support.

CHAPTER 1 - Introduction

Biometrics is a method for recognizing an individual based on the physiological or behavioral characteristics. Fingerprints, DNA, palm, face, iris, vein and retina are some of the examples of physiological characteristics. Handwriting, gait, speech and signature are few behavioral characteristics. In general a biometric system consists of seven components: a sensor that collects and converts the data to digital; pre-processing algorithms that remove artifacts from the digital output obtained from the sensor. These algorithms usually enhance, segment, normalize the digital images from the sensor; a feature extractor that extracts significant features; a template generator that generates a biometric template which provides a discriminating representation of features; a storage component or the database that stores templates; a classifier that compares the generated template with the other stored templates for recognition. This result will be used for various applications.

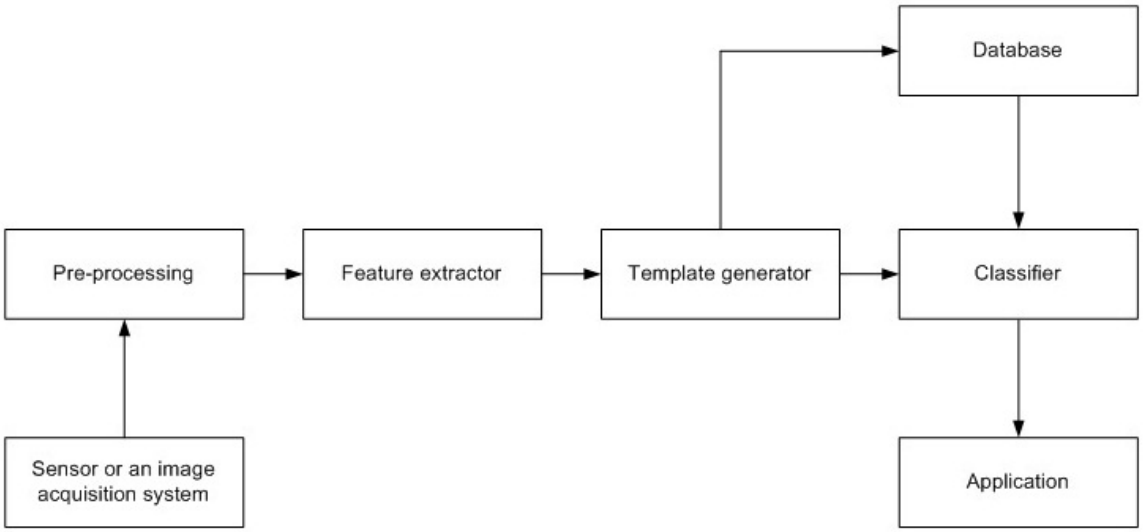

Figure 1.1 Basic Block diagram of Biometric System

Fingerprint recognition is a technique developed for identifying an individual based on the fingerprint patterns. Analysis of fingerprints requires comparison of several features like ridges and minutia patterns. Fingerprint recognition is performed by involving the users to place their fingers on the platen of biometric device for the fingerprint to be read electronically and then the vendor's algorithm extracts the above mentioned features. Retinal recognition is a biometric technique that compares the patterns existing on retina. A retinal scan is performed by

subjecting a low-energy infrared light ray into a person's eye as they look through the light source of the biometric device. The results of the scan are converted to computer code and stored in a database. Hand geometry is one of the commercial biometric products where the system scans an individual's hand. Dimensions of the hand are measured and compared to those collected during enrollment. Speech recognition uses vocal characteristics to recognize individual's speech [13]. Telephone or a microphone serves as a sensor that makes it a cheap technology. Signature recognition measures the speed, direction and the pressure one applies while signing his or her name. Face recognition is the complex biometric recognition. A facial recognition system is an application that identifies or recognizes the person from a digital image or a video frame. Despite the volumes of research, there are no proper methods for automated face recognition as there are for fingerprints and iris.

Iris recognition is a method of recognizing a person by analyzing the iris pattern. Iris patterns of identical twins differ and a person's left and right eyes have different patterns as well. It is regarded as the most reliable biometric technology since iris is highly distinctive and robust [11]. The current and the future applications of this technology include a substitute for passports at secured and restricted areas in airports; screening at border crossings; database access and computer login; secure access to bank accounts at ATM's and credit card authentication; driving license registration and for biometrically enabled National Identity Cards. Several airports worldwide have installed the iris recognition system for screening the passengers at immigration control. Most of these commercial iris recognition systems use algorithms developed by Daugman [1], since these algorithms are able to extract the iris region from an eye image with good recognition rate.

Iris is a strong contender to face and fingerprints. Coding for the iris templates in iris recognition originated from Daugman's system that used Gabor wavelets [2]-[4]. Wildes [5] and Boles [6] also contributed for iris recognition in their works respectively. Government organizations are carrying out research in this area as a result of recent expiry of the key patents and this led to the improvements in the image acquisition (sensor), preprocessing, feature extraction and matching stages [7]-[10]. In this report, techniques for recognizing iris will be discussed in detail.

1.1 Motivation

In the current methods, iris recognition relies on feature extraction. Improper selection of features may result in the wrong classification of the iris images. Lots of work has been done in the past on iris recognition, but most of the algorithms are complex and consume more time. In Daugman's algorithm [2], the iris image is filtered using Gabor filters. The phase structure is then demodulated into complex phasors to generate binary iris code [2], [3]. Ma of the Chinese Academy of Sciences Institute of Automation and Libor Masek of University of Western Australia implemented Daugman's algorithm for the CASIA database. Tan [12] in his work used a class of wavelets to filter the 1D intensity signals generated from the iris images. The position of the generated vibrations is recorded in the form of a feature vector. For all the above algorithms, the preprocessing stage of iris localization and normalization is common. This stage has a segmentation subsystem that localizes the iris region from an eye image and isolates eyelids, eyelashes. Circular Hough transform is used for detecting the iris-sclera boundary and iris-pupil boundary, and the linear Hough transform for detecting the eyelids. The segmented iris pattern is normalized by remapping each point (Cartesian coordinates) of the iris to the polar coordinates. This is achieved by creating a rectangular image array that will be mapped to a radial and angular position in the iris [10]. Daugman's rubber sheet model is used to unwrap the iris region to a rectangular block of constant dimensions. Feature encoding and matching stages of an iris recognition system are different in each of the above mentioned algorithms. To improve the performance in terms of feature extraction time, complexity and recognition rate, new methods are proposed in this report for encoding only significant features of the iris template and making the comparisons between these templates, so that a decision can be taken as to whether the templates are generated from the same person or from different persons [11].

1.2 Organization

The rest of the report is organized as follows. Chapter 2 will detail the general steps involved in the iris recognition system. Chapter 3 introduces the proposed methods for recognizing iris and explains the steps in these methods with a block diagram. The experimental results of the proposed methods are shown in Chapter 4. Finally, we conclude the report in chapter 5, with suggestions for possible future research and extensions to the present work.

CHAPTER 2 - Iris Recognition

2.1 Iris

Iris is a thin membrane that is located between cornea and lens of the human eye. The average diameter of human iris is 12 mm and the size of pupil changes from 0.1 to 0.8 of the iris radius. The front view of the human eye from the CASIA database is shown in the figure 2.1. Iris is responsible for controlling the amount of light reaching the pupil. It consists of two layers; stroma and beneath the stroma is the epithelium layer. Stromal layer consists of blood vessels, two iris muscles and pigment cells. Epithelium layer consists of pigmented epithelial cells. The color of iris is determined by the density of stromal pigmentation.

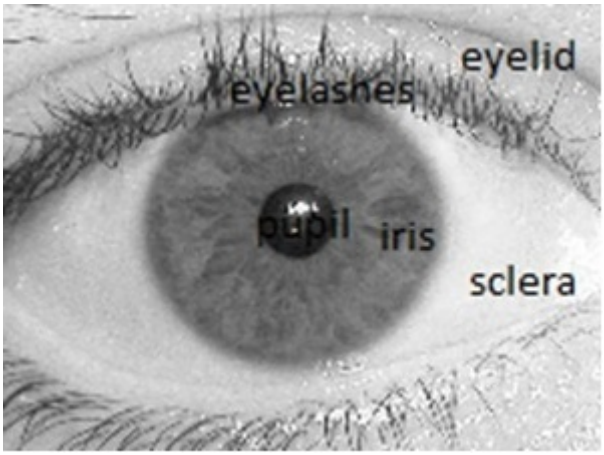

Figure 2.1 Front view of Human eye

Iris formation begins during the third month of gestation [14] and the structures creating the iris patterns are completed by the end of first year of human life whereas; stromal pigmentation takes place for the first few years. The formation of unique iris patterns is not related to any genetic factors [5]. Iris pigmentation which determines color is the only characteristic that is dependent on genetics. The epigenetic nature of iris patterns result in independent patterns for the two eyes of an individual and uncorrelated patterns for identical twins.

2.2 Iris Recognition System

Iris is a well protected organ that is visible externally. Its epigenetic patterns remain stable throughout the life. This characteristic of iris makes it to be used as a biometric for

recognizing individuals. Digital image processing techniques are employed to extract iris from the digital eye image and encode it into a biometric template. This biometric template provides a discriminating representation of features which will be compared to the other stored templates and recognized by a classifier. When a person has to be recognized by an iris recognition system, a photograph of their eye is taken and then an iris template is created from the eye image. This template is compared with the other stored templates until a matching template is found and the person is identified; or no match is found and the person remains unidentified [11].

The main objective of this report is to implement an iris recognition system and verify its performance. The development tool used is MATLAB with the emphasis only on the software for performing iris recognition. To test the system, CASIA database [15] of 756 digitized grayscale eye images and the UBRIS.v1 database [19] of 1877 images are used.

Iris recognition system is composed of several subsystems. These subsystems include segmentation – localizing the iris region in an eye image, normalization – creating a rectangular block of iris pattern from the circular iris region to eliminate dimensional inconsistencies, feature encoding – generating a template containing only the significant features of the iris region, matching and classification-measuring the similarity between two iris templates. The overall performance of an iris recognition system is highly related to the proper design of its subsystems.

2.3 Segmentation

Segmentation is the first stage of an iris recognition system that isolates the iris region in an eye image by locating pupil, two eyelids and eyelashes that may cover some areas of the iris texture. The iris region is isolated by approximating two circles, one for the iris-pupil boundary and the other for iris-sclera boundary as shown in figure 2.2. The eyelids and eyelashes that are located on the upper and lower parts of the iris also need to be eliminated from the circular iris region. This is the crucial stage in the iris recognition system since data that is wrongly represented as iris will corrupt the generated biometric template, and this would result in poor recognition rate. The success of segmentation depends on the quality of eye images considered for research. Some of the algorithms that are designed to isolate the iris region in an eye image are mentioned below.

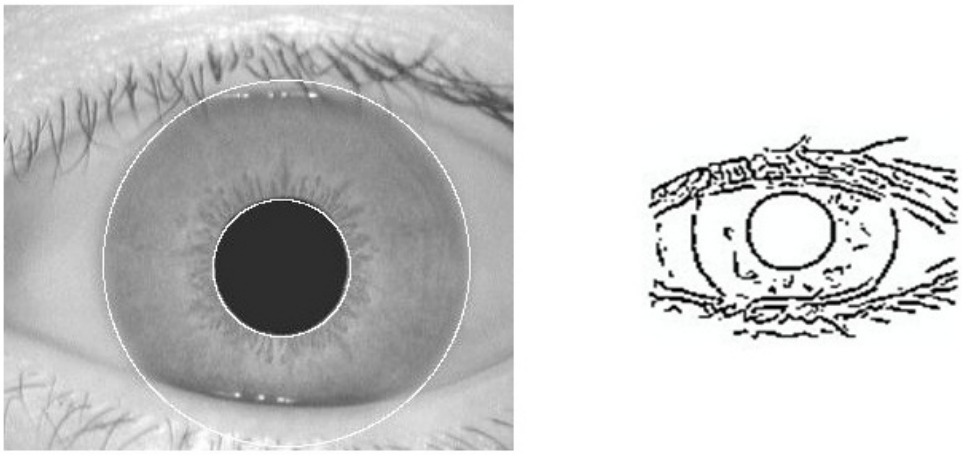

Figure 2.2 Segmented eye image and the edge map with two approximated circles [11]

2.3.1 Hough Transform

It is an algorithm used to compute the parameters of the geometric objects (lines and circles) in an image. This feature extraction technique is used in image analysis and digital image processing to find shapes of the objects by a voting procedure within the classes available. Circular Hough transform can be used to find the center coordinates and radius of the iris and pupil regions. In the segmentation algorithm, an edge map is created by computing the gradients (first derivatives of intensity values) in an eye image. For each edge pixel in the edge map, the surrounding points on the circle at different radii are taken and votes are cast for finding the maximum values that constitute the parameters of circles in the Hough space. The center coordinates and the radius are computed using the following equation.

$$x^2 + y^2 - r^2 = 0 \qquad (2.1)$$

The maximum point corresponds to the radius 'r'; the center coordinates (x, y) of the circle are given by the edge points in the Hough space. Parabolic Hough Transform and linear Hough transform can be used to detect the upper and lower eyelids.

To perform the edge detection, derivatives (gradients) are taken in the vertical direction for detecting the iris-sclera boundary, in order to reduce the influence of the eyelids that are horizontally aligned. For detecting the eyelids, gradients are taken in the horizontal direction. This method localizes the iris boundary accurately, since less number of edge points (not all edge pixels) is taken into account to cast votes in Hough space.

Even though the circle localization is accurate, there are some problems in using Hough transform. This method requires threshold values for detecting edges and any improper threshold values may lead to the false detection of the iris region. Hough transform is only efficient if majority of votes fall into the right bin, so that the bin is detected accurately by avoiding the background noise. Efficiency of the Hough transform depends on the edge detection and also on the quality of the input images considered.

2.3.2 Daugman's Integro-differential operator

Integro-differential operator is used for estimating the center coordinates and radius of iris and pupil regions. Eyelids can also be localized using this operator by changing the path of the integral from circular to an arc using the statistical estimation methods. The integro-differential operator given by Daugman [1] is defined as

$$\max_{(r,x0,y0)} \left| G_\sigma(r) * \frac{\partial}{\partial r} \oint_{r,x0,y0} \frac{I(x,y)}{2\Pi r} ds \right| \qquad (2.2)$$

where I(x, y) is the image, r is the radius, $G_\sigma(r)$ is a Gaussian function with the scale σ, s is the contour of the circle. The operator * searches for the path where maximum change occurs in the pixel values (x, y) by varying radius r and the center coordinates of the normalized contour integral of I(x, y).

Similar to the Hough transform, Daugman's integro differential operator also makes use of the first derivatives of the image and searches for the geometric parameters. But Daugman's operator does not suffer from the thresholding problems as the Hough transform does, since it deals with the raw derivative information.

2.3.3 Adaptive Thresholding

Thresholding is a technique used generally for detecting eyelashes, since they are dark compared to the surrounding regions. If the intensity value is less than the threshold value then the point belongs to the eyelashes. Eyelashes are of two types, separable eyelashes and multiple eyelashes that are grouped together. Separable eyelashes are detected using Gabor filters. If the resultant point is less than the threshold value then the point belongs to the eyelash. Multiple eyelashes are detected by calculating the variance of intensity. If the variance is less than the threshold, the center is taken as the point in the eyelash.

2.3.4 Contour Models

Contour models are used for localizing the pupil in eye images. These models detect pupil using two defined forces: internal and external forces. The contours respond to these forces by deforming the image internally or moving across an image until equilibrium is achieved [11]. The contour consists of vertices whose positions can be changed by these forces. The internal forces expand the contour to a polygon with radius δ and the external forces which are obtained from the grey level intensity values of the image push the vertices inward. The internal force F_{int} and the external force are G_i given by

$$F_{\text{int}} = V_i - U_i \qquad (2.3)$$

$$F_{ext,t} = I(U_i) - I(U_i + F_{ext,t}) \qquad (2.4)$$

where V_i is the expected position of the vertex in the polygon. $I(U_i)$ is the grey level of the nearest neighbor to U_i. The movement of the contour depends on both the internal and external forces over the contour vertices. Each vertex is moved between t and t+1 and this is given by

$$U_i(t+1) = U_i(t) + F_{\text{int},t} + F_{ext,t} \qquad (2.5)$$

where U_i is the position of vertex I, F_{int} is the internal force, F_{ext} is the external force. For localizing pupil, the internal forces are calibrated so that the contour forms an expanding discrete circle [11]. The external forces are calculated using the edge information.

2.3.5 Other Segmentation Algorithms

Other researchers used methods similar to the described segmentation methods. The segmentation algorithm proposed by Tisse et al. [8] uses integro-differential operator and the Hough transform. The Hough Transform is used for detecting the center of pupil and integro-differential operator is used to locate pupil boundary accurately. Lim et al. in his work located pupil by creating an edge map of the intensity values of the image. The center of pupil is obtained by casting votes for the point that has large number of perpendicular line crossovers [9].

2.4 Normalization

After segmenting the iris region in an eye image, the next step is to unwrap it into a rectangular block of fixed dimensions. Dimensional inconsistencies occur in these images. These inconsistencies are mainly due to the stretching of the iris caused by dilation of pupil. Imaging distance, head tilt, rotation of the eye within the socket and rotation of the camera are some of

the sources of inconsistency. There are various methods for normalizing the iris region so that it has fixed dimensions. Some of the methods are listed below.

2.4.1 Daugman's Rubber Sheet model

Daugman's rubber sheet model transforms the iris region from Cartesian coordinates to polar coordinates (r, Θ) where r lies in the interval of [0, 1] and Θ is in the range of [0, 2Π].The normalization process is dimensionless in the angular direction (Θ) and changes linearly in the radial direction (r).The remapping of iris region from Cartesian to polar coordinates [11] is given by

$$I(x(r,\theta), y(r,\theta)) \rightarrow I(r,\theta) \qquad (2.6)$$

where

$$x(r,\theta) = (1-r)x_p(\theta) + rx_i(\theta)$$

$$y(r,\theta) = (1-r)y_p(\theta) + ry_i(\theta)$$

I(x, y) is the iris image where (x, y) are the Cartesian coordinates and (r, Θ) are the polar coordinates; x_p and y_p are the pupil coordinates and x_i and y_i are the iris coordinates along the direction of Θ. The normalization process takes pupil dilation and size inconsistencies into account to produce normalized representation of iris region. The normalization of iris region is shown in the figure 2.3 with pupil center as the reference point.

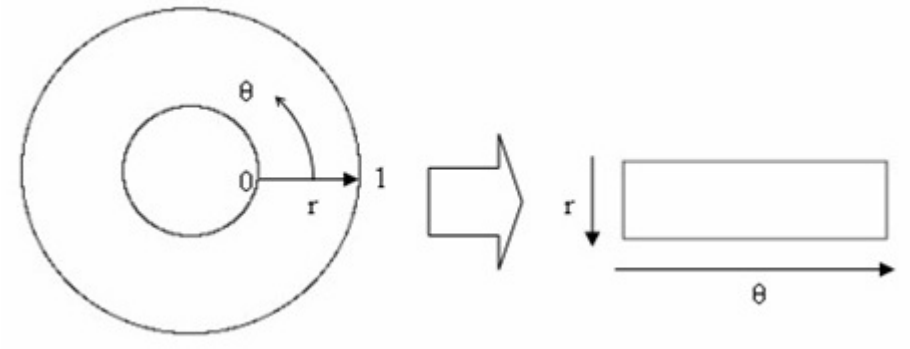

Figure 2.3 Daugman's Rubber sheet model [11]

2.4.2 Image Registration Technique

Wildes [5] proposed an image registration technique for normalizing the iris region. In this model, a newly acquired image I_a (x, y) would be aligned with an image in the database I_d(x, y) so that these images can be compared. The intensity values of the new image are made closer to

the corresponding points in the reference image using the mapping function (u(x, y), v(x, y)). The mapping function is chosen to minimize

$$\iint (I_d(x,y) - I_a(x-u, y-v))^2 dxdy \qquad (2.7)$$

This alignment process compensates the rotation and scale variations. The mapping function is given to transform the image coordinates. Wildes's normalization process is slightly different from the Daugman's method. Daugman's method consumes more time for recognition and could not compensate the rotation variations whereas; image registration technique compensates the unwanted factors such as scale and rotation variations.

2.4.3 Other Normalization methods

Lim et al. uses a method similar to the Daugman's method. In this method after finding the pupil center and the inner and outer boundaries of iris, the iris texture is transformed to polar coordinates with a fixed resolution. In the radial direction (r), the texture is normalized from the inner boundary to the outer boundary into 60 pixels which is fixed for all the iris images. The angular resolution (Θ) is also fixed to a 0.8 degree over the 360 degree which produces 450 pixels in the angular direction [9]. Boles normalization technique is similar to Daugman's method except that it is performed at the time of matching. This method is based on the diameter of the two matching irises.

2.5 Feature Encoding

The most significant information of the iris texture must be extracted as features, to provide accurate recognition and to make comparisons between the templates. Previous works used the following feature encoding algorithms:

2.5.1 Wavelet Encoding

Wavelet is one of the transforms that constructs a time-frequency representation for continuous time signals. Wavelet transforms a signal to a different domain using filter banks. Wavelet transform can be applied over the normalized iris region to decompose it into components that occur at different resolutions. The output is then encoded in order to extract the most significant information.

2.5.2 Gabor Filters

A Gabor filter is a linear filter whose impulse response is given by multiplying a harmonic function with a Gaussian function. A signal is decomposed using a pair of Gabor filters; with the real part given by modulating a cosine wave with Gaussian wave and the imaginary part given by modulating a sine wave with Gaussian wave. The center frequency of the filter is given by frequency of the sine wave or cosine wave. Daugman used a 2D version of Gabor filters [1] to encode the iris texture. A 2D Gabor filter [11] over an image domain (x, y) is given by

$$G(x,y) = e^{-\Pi[(x-x_0)^2/\alpha^2+(y-y_0)^2/\beta^2]} e^{-2\Pi i[u_0(x-x_0)+v_0(y-y_0)]} \qquad (2.8)$$

where (x_0, y_0) specifies position in the image, (α, β) specifies the width and length, and (u_0, v_0) specify modulation. Daugman demodulated the output of the Gabor filters by quantizing the phase information into four levels, one for each quadrant. These four levels were represented by two bits of data, so that each pixel corresponds to two bits of data in the iris template. Daugman used polar coordinates for normalizing the template, as only phase information is required for encoding the most significant features in the iris.

2.5.3 Haar Wavelet

Haar wavelet transform is the simplest wavelet used to extract features from the iris region. Gabor wavelet and Haar wavelet are the mother wavelets. In case of iris recognition, Lim et al. [9] in his work proved that Haar wavelet provides slightly better recognition rate when compared to Gabor wavelet. Haar wavelet function ψ(t) and its scaling function φ(t) are defined as

$$\psi(t) = \begin{cases} 1 & (0 < t < 1/2) \\ -1 & (1/2 \le t < 1) \\ 0 & \text{otherwise} \end{cases}$$

$$\varphi(t) = \begin{cases} 1 & (0 \le t < 1) \\ 0 & \text{otherwise} \end{cases}$$

2.5.4 Log- Gabor Filter

Gabor filters are used to obtain frequency information. They provide localization of both space and frequency information. But the bandwidth of Gabor filter is limited to one octave and also it has a dc component when the bandwidth is more than one octave. In order to obtain the

zero dc component for any bandwidth, Gabor filters are used on a logarithmic scale known as a Log- Gabor filter.

2.5.5 Gaussian Filters

To encode the most discriminating features, Wildes et al. [5] decomposed the iris template by applying the Laplacian of Gaussian filters to the iris region. These filters are defined as

$$\delta G = \frac{1}{\Pi\sigma^4[1-\frac{\rho^2}{2\sigma^2}]e^{\frac{-\rho^2}{2\sigma^2}}} \qquad (2.9)$$

where σ is the standard deviation of the Gaussian, ρ is the radial distance from the center of the filter. The filtered image is then represented as a pyramid that compresses the data by having only significant information.

2.6 Matching and Classification

The template generated in the feature extraction stage needs a matching metric to measure the similarity between two iris templates. This metric gives one range of values when templates generated from the same eye (intra-class distribution) are compared and another range of values when templates generated from different person eye's (inter-class distribution) are compared. These two distributions should give distinct hamming distance values; so that we can decide as to whether the two templates belong to the same or different persons. Some of the common matching algorithms are listed below:

2.6.1 Hamming distance Classifier

Hamming distance is generally used for detection and correction of errors in digital image processing. It is a matching metric employed by Daugman to measure the similarity between two iris templates. It gives the number of bits that are same in two iris patterns. Using the hamming distance, a decision can be taken as to whether the two templates belong to the same or different persons. To calculate the similarity between two patterns A and B, the hamming distance HD, is given by

$$HD = \frac{1}{N}\sum_{i=1}^{i=N} A_i (XOR) B_i \qquad (2.10)$$

where N is the total number of bits in the iris pattern. Each iris generates a bit- pattern that is independent to the pattern generated from another iris since; each individual's iris region contains features with high degrees of freedom [11]. Iris codes generated from the same iris are highly correlated. If two iris templates are completely independent, the hamming distance between the two patterns should be high and if the two bit patterns are from the same eye, the hamming distance should be low.

2.6.2 K-Nearest neighbor classifier (Euclidean distance)

K-Nearest Neighbor is the simplest of all classifiers that classifies objects based on the nearest training neighbors in the feature space. It uses Euclidean distance as a distance metric. This classifier can be used to compare two templates, especially if the template is composed of integer values. Object is classified or recognized based on the majority number of its neighbors, and is assigned to the class that is most common among its k nearest neighbors. If 1-nearest neighbor is considered, then the object is assigned to the class of its first nearest neighbor; generally larger values of k are considered to reduce the effect of noise on the classification. In terms of Euclidean distance, the difference, d between the M descriptions of a sample, s is given as

$$d = \sqrt{\sum_{i=0}^{i=m} (s(i) - k(i))^2} \qquad (2.11)$$

2.6.3 Correlation Classifier

Wildes et al. [5] used the correlation classifier to find a match between the image acquired and the images in the database. This was given by:

$$d = \frac{\sum_{i=1}^{i=n} \sum_{j=1}^{j=m} (p_1[i,j] - \mu_1)(p_2[i,j] - \mu_2)}{nm\sigma_1\sigma_2} \qquad (2.12)$$

where p_1 and p_2 are two images of size n x m, μ_1, μ_2; σ_1, σ_2 are the means and standard deviations of p_1 and p_2 respectively.

CHAPTER 3 - Current Methods for Iris Recognition

In the current methods of iris recognition, segmentation and normalization stages are common (same). In the segmentation stage, iris region is isolated in an eye image by eliminating eyelids, eyelashes. The segmented iris region is normalized using Daugman's rubber sheet model in the normalization stage. In the first method, Wavelet transform is applied to the iris template for extracting significant features since it has plenty texture information. K-Nearest neighbor classifier is used to classify the templates (feature vectors) generated in the feature extraction stage. This classifier finds the nearest neighbors to the test image in the feature space.

The second method proposed by Jong-Gook Ko, Youn-Hee Gil, Jang-Hee Yoo, Kyo-IL Chung [18] employs a cumulative sum based analysis for extracting features and generates iris codes for the template by the proposed code generation algorithm. Hamming distance classifier is used to measure the similarity between two iris templates. Detailed description of these methods is discussed in the sections below.

3.1 Segmentation Stage

The iris region is localized in an eye image using the segmentation algorithm mentioned in the Libor Masek's thesis [11]. In this algorithm, an eye image is sent as an input to the segmentation system to localize the iris region by finding the pupil, two eyelid boundaries and the eyelashes. The range of the radius of pupil and iris are set manually for the CASIA data base and UBRIS.v1 database, since these values vary for each database. To detect the iris and pupil boundaries accurately, Circular Hough transform is applied first to the iris-sclera boundary and then to the iris-pupil boundary, since pupil lies within the iris region. It involves canny edge detection for generating an edge map. In performing the edge detection, gradients are biased in the vertical direction for the iris- sclera boundary; and in horizontal and vertical direction for the iris-pupil boundary. From the gradient image, weak edges are eliminated by thresholding. If the intensity values are greater than the high threshold then those pixels are considered as edges and if the intensity values are less than the lower threshold, then those pixels are considered as weak edges and eliminated. If the intensity values lie between the high and low threshold, then the average of its neighboring pixels is taken and if the value is greater than the lower threshold, then

the pixel is considered as the edge point. After eliminating weak edges, radius and centre coordinates for iris and pupil are calculated from the edge map by applying circular Hough transform.

Eyelids were isolated by drawing a line to the upper and lower eyelids using the linear Hough transform. A second horizontal line is then drawn intersecting the first line at the edge of the iris that is closest to the pupil, to isolate maximum of eyelid regions. These lines lie exterior to the pupil and interior to the iris. This process is shown in Figure 3.1 and is done for both the eyelids (top and bottom). Canny edge detection is used for generating an edge map and only horizontal gradient information is taken for detecting the eyelids. Linear Hough transform or parabolic Hough transform can be used to detect the upper and lower eyelids. But parabolic Hough transform requires more parameters to deduce. Therefore, linear Hough transform is used to detect the eyelids. If the maximum value in the Hough space is less than the threshold, then no lines are drawn. For isolating eyelashes, a simple thresholding technique is used, since eyelashes are dark when compared with the rest of the eye image.

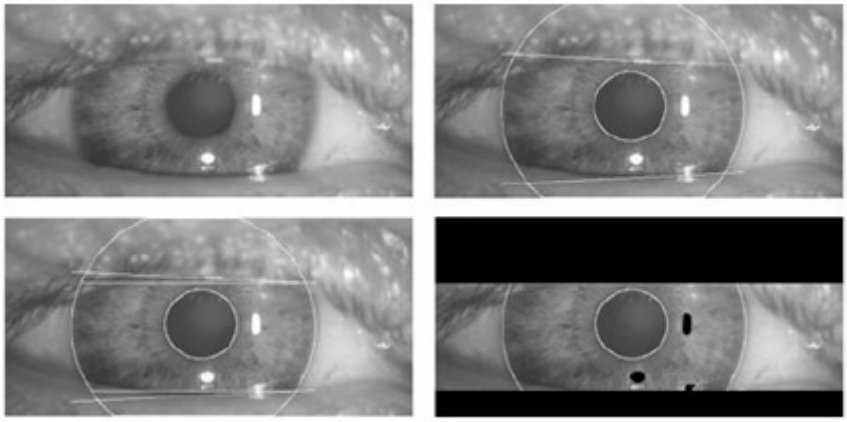

Figure 3.1 Stages of Segmentation [11]

3.2 Normalization Stage

Once the iris region is localized in an eye image, the next stage is to normalize the circular iris region to a rectangular block so that it has fixed dimensions. This is achieved using Daugman's rubber sheet model mentioned in the Libor Masek's thesis [11]. In this model, each point of the iris region is remapped to a pair of polar coordinates (r, θ).

For normalization, radial vectors are drawn over the iris region with center of the pupil as the reference point. A constant number of data points are considered on each radial line for all

the segmented eye images and this is referred as radial resolution. The number of radial lines in the iris region is defined as angular resolution. If pupil is non-concentric to iris, a remapping formula is required to rescale points on pupil depending on the angle around the circle. The remapping formula is given by

$$r' = \sqrt{\alpha\beta} \pm \sqrt{\alpha\beta^2 - \alpha + r_I^{\,2}} \qquad (3.1)$$

where

$$\alpha = o_x^2 + o_y^2$$

$$\beta = \cos(\Pi - \tan^{-1}(\frac{o_y}{o_x}) - \theta)$$

where α is the displacement of the center of pupil relative to the center of iris; r' is the length of the radial vector in terms of angle Θ; r_I is the iris radius. A constant number of points are taken along each radial line irrespective of the radius (low or high) at a particular angle. To find the Cartesian coordinates of the data points in the angular and radial direction, a normalized pattern is created. From the dough nut region shown in the figure 3.3, normalization generated a 2D array with angular resolution (Θ) in horizontal dimensions and radial resolution (r) in vertical dimensions. To prevent the corruption of normalized pattern from the non iris data, data points along the pupil border are discarded. Normalization stage proved to be successful and resulted in rectangular templates of size 20x240 for both the databases.

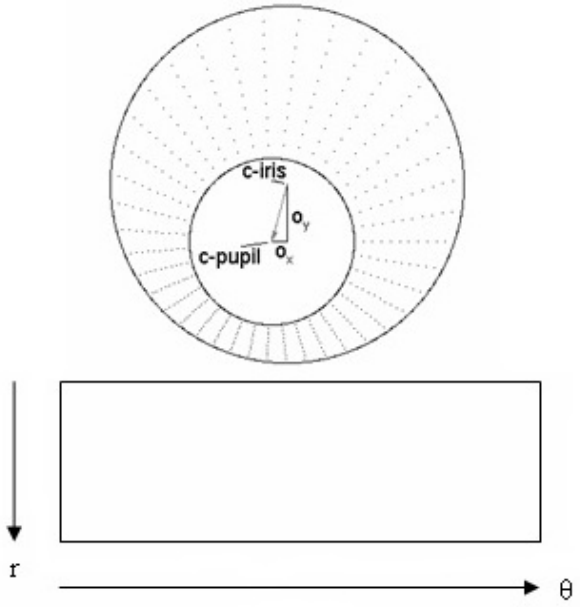

Figure 3.2 Normalization pattern with angular resolution and angular resolution [11]

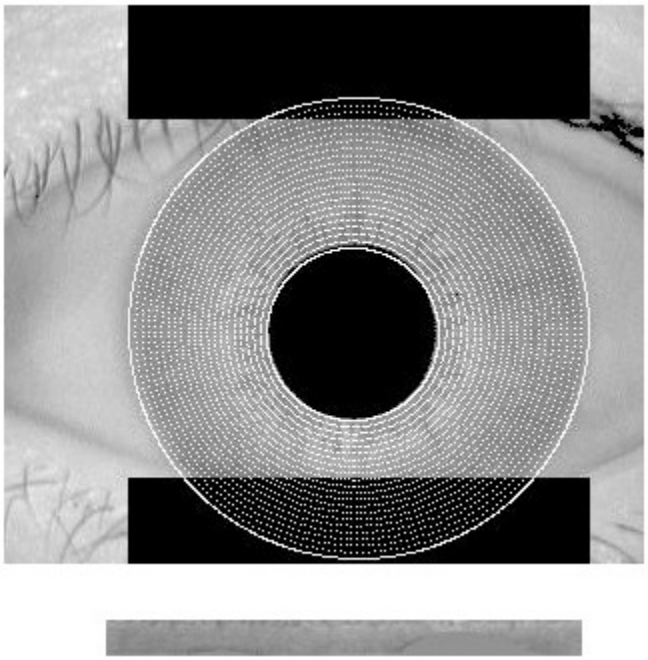

Figure 3.3 Normalization of CASIA eye image

3.3 Iris Recognition using Wavelet Transform

In order to provide accurate recognition, the most discriminating information present in the iris pattern must be extracted and only significant features must be encoded so that iris images are recognized properly. In the current method, energy is the feature extracted from the transformed image and in order to select the significant features and form a feature vector, variance is computed. After obtaining the feature vector for each iris image, K-nearest neighbor classifier is used to classify or recognize these iris images. Detailed information of feature extraction and matching stages of the current iris recognition system is described below.

3.3.1 Introduction to Wavelet Transform

Wavelet is a signal transform that transforms the signal to a different domain, performs some operation on the transformed signal and then inverse transforms it back to the original domain. This transform is invertible; the reconstruction of signal should be perfect in case of no data processing. This condition holds good in case of the wavelet transform. Continuous wavelet transform of a signal f(x) is given by

$$CWT(a,\tau) = \frac{1}{\sqrt{a}} \int_{-\inf}^{+\inf} f(x)\psi(\frac{x-\tau}{a})dx \qquad (3.2)$$

where ψ is a base wavelet, the parameters a and τ are the scaling parameter and shift parameter respectively . A simple one-stage filter bank is shown in the figure 3.4 and it uses FIR filters. IIR filters cannot be used since their infinite response leads to infinite data expansion and also the output data stream will be cut resulting in the loss of data. The one-stage wavelet transform uses two analysis filters, a low-pass filter g1 and a high-pass filter h1, to filter the data. The filtered data is down sampled in the forward transform. In the inverse transform, the signal is reconstructed by up-sampling and then using two syntheses filters, a low-pass filter g and a high-pass filter h. Filters are necessary since, up-sampling is done by inserting a zero in between every two samples and the filters smoothen the response.

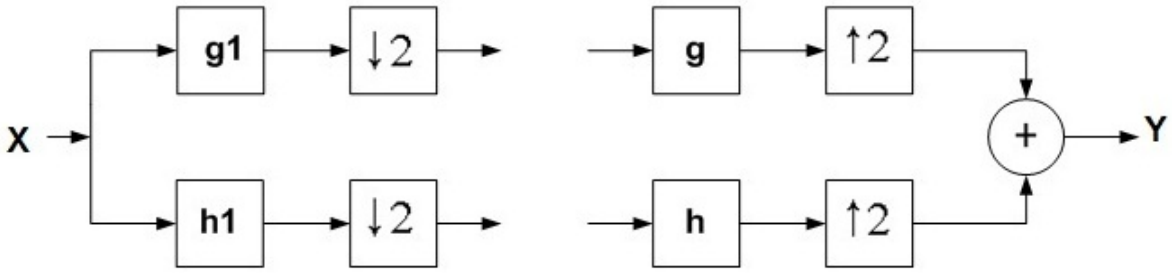

Figure 3.4 One-Dimensional Wavelet Transform

The 2-D wavelet transform is shown in the fig 3.5. For an image, 1-D wavelet transform is applied to the rows and columns. The resultant is created by passing the image through filter banks. The filtered signal is down sampled in horizontal (rows) and vertical (columns) direction. The image is then decomposed into sub bands, LL, LH, HL, and HH. LL sub band contains the original image with half resolution. LH and HL sub bands contain the edges of the image. HH band contains the high frequency details. There are several filters for wavelet transform, for example, Haar, Daubechies etc.

Lifting wavelet transform is a technique used to construct DWT using lifting steps. In this process, the signal is split into odd and even samples. In the predict step, odd samples are predicted from the even samples. In the update step, even samples are updated from the input even samples and updated odd samples. Forward Lifting transform is described in the figure 3.6. Advantages of lifting wavelet over other transforms:

1. Lifting process speeds up the process when compared to the standard implementation.

2. Lifting transform does not require additional memory since transformation takes place in the memory of the input data.

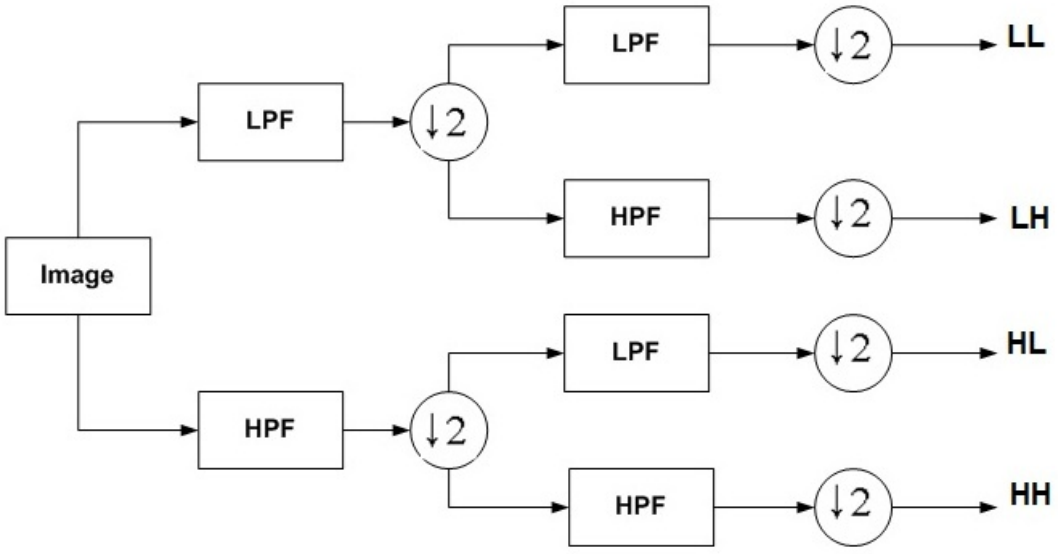

Figure 3.5 Two-Dimensional Wavelet Transform

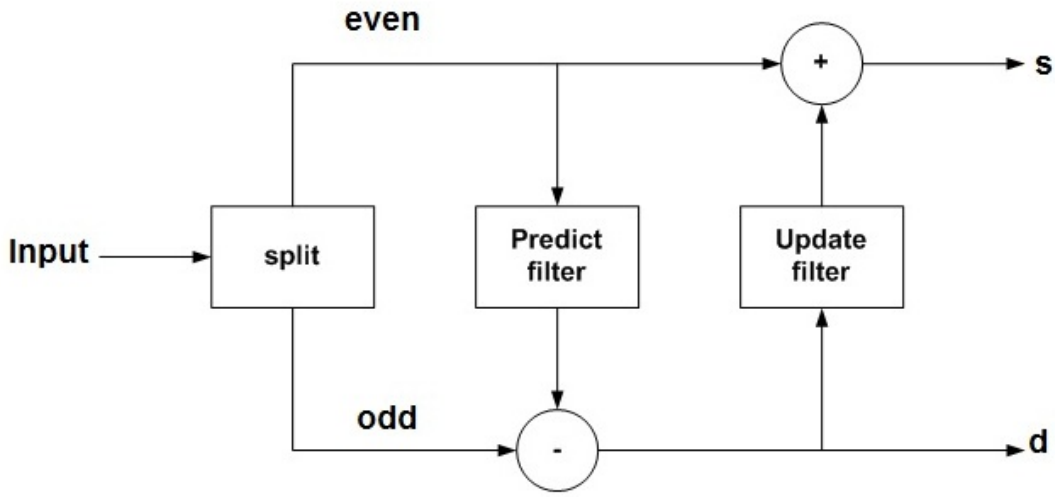

Figure 3.6 Forward Lifting Wavelet Transform

3.3.2 Feature Extraction Stage using Lifting Wavelet Transform

In order to provide accurate recognition of individuals, only the most significant features must be encoded so that templates can be compared. The iris template has been divided into 20X20 blocks and Lifting Wavelet transform is applied to each block. Each block is divided into 4 sub bands denoted by LL, LH, HL, and HH.

$$FP(u,v) = LWT(P(u,v)) \qquad (3.3)$$

where FP (u, v) and P (u, v) are the transform and pixel data respectively. The transform data is normalized by calculating the sum of the squared values of each magnitude component (except the zero frequency components), so that the magnitude data is invariant to shifts in illumination. Normalization coefficients are given by NFP.

$$NFP(u,v) = \frac{abs(FP(u,v))}{\sqrt{\sum FP(u,v)^2}} \qquad (3.4)$$

The transformed data is then described by energy, e. This measure is immune to rotation and is scale invariant. Other measures such as energy in the major peak, Laplacian of the major peak, entropy, inertia, largest horizontal frequency and largest vertical frequencies can also be considered as the features. Energy is computed for the iris template using the formula

$$e = \sum_{u=1}^{m}\sum_{v=1}^{n} NFP(u,v)^2 \qquad (3.5)$$

The size of each template is 20x240. Each template has been divided into 12, 20x20 blocks and each 20x20 block has been divided into 4 sub bands. Therefore a feature vector (by computing the energy) of size 1x48 is obtained for each iris template. By repeating the procedure for the entire data set of the images, we get several energy feature vectors of length 1x48. In order to select significant features from the iris template, variance is computed. The energy values corresponding to the 10 largest variance values are taken for each iris image to form a feature vector for each iris image.

3.3.3 Matching Stage using K-Nearest Neighbor

Once the feature vectors are obtained, they are classified using the k nearest neighbor classifier. The main purpose of this classifier is to find an object in the database that best matches with the test sample. Object is recognized based on the majority number of its neighbors, and is assigned to the class most common among its k nearest neighbors. It uses Euclidean distance as a distance metric. This Euclidean distance between the test image and the training images (iris templates) in the database is computed using the following equation. Based on their distances, the iris templates are classified.

$$d = \sqrt{\sum_{i=0}^{i=m} (Test(i) - training(i))^2} \qquad (3.6)$$

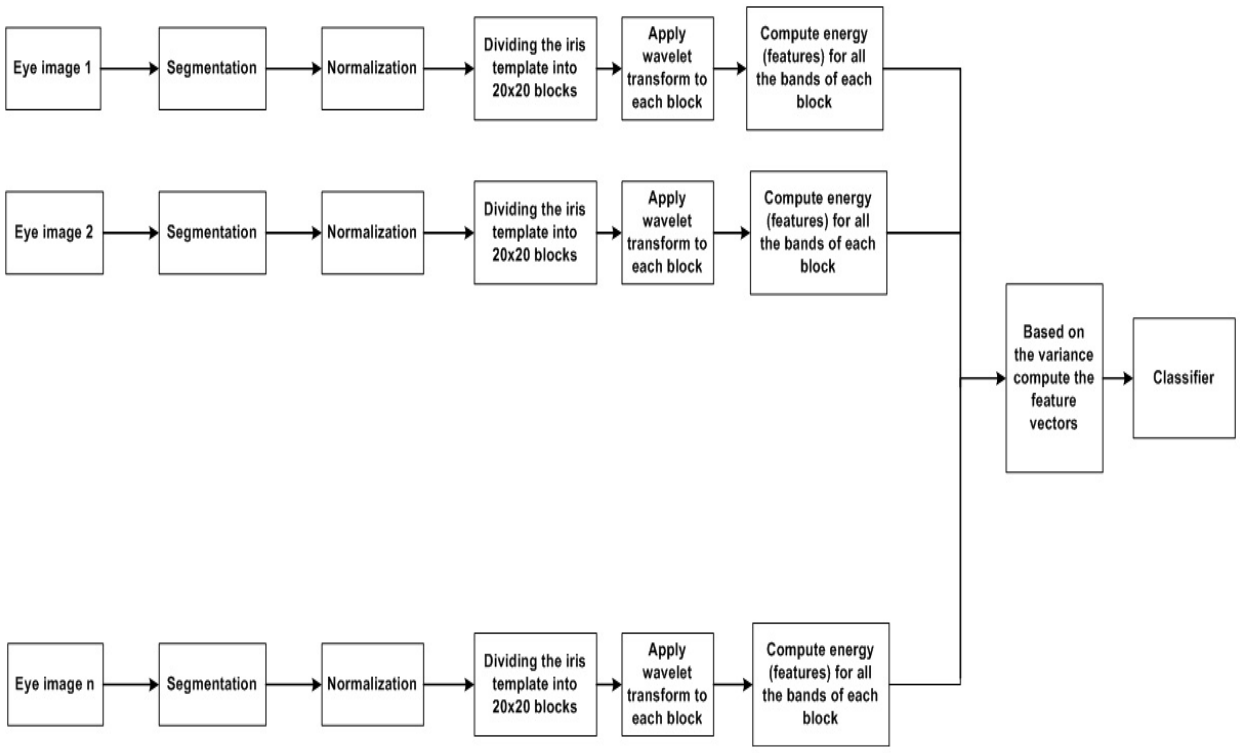

Figure 3.7 Block diagram of the iris recognition system using wavelet transform for extracting features

3.4 Iris Recognition using Cumulative Sum Based Analysis

The iris region is localized in an eye image using the Segmentation algorithm mentioned in the section 3.1. The segmented iris region is then normalized using the Normalization algorithm mentioned in the section 3.2. In this method, feature encoding is done using the code generation algorithm.

3.4.1 Feature Encoding Stage

In order to provide accurate recognition of individuals, only the most significant features must be encoded so that rectangular templates can be compared. A cumulative-sum-based analysis method given by Jong-Gook Ko, Youn-Hee Gil, Jang-Hee Yoo, Kyo-IL Chung [18] is used to extract features from the iris templates. In this method, the normalized iris template is divided into cells for calculating cumulative sums. Each cell is of 5x20 pixels size. An average grey value of the cell is used to represent each cell. These cells are grouped horizontally and vertically as shown in the figure 3.8(four cell regions are grouped together) to describe the grey

value variations. Then cumulative sums are calculated in the following way. Let's assume X1, X2, X3, X4 are the average grey values of the four cell regions within first group.

1. The average of all the four cells within a group, X_m=(X1+X2+X3+X4)/4 is calculated.

2. Cumulative sums for the cells within the group are computed from 0 with S (0) =0. The cumulative sums for the other cells are computed by adding the previous sum to the difference between the current cell value and the average value.

$$S(i) = S(i-1) + (X(i) - X_m) \qquad \text{For i=1, 2, 3, 4} \qquad (3.7)$$

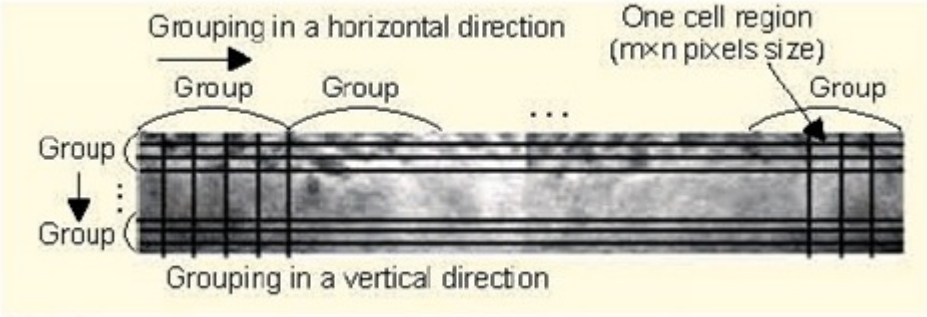

Figure 3.8 Iris template is divided into cells and grouped horizontally and vertically [18]

After calculating the cumulative sums for the horizontal and vertical groups, iris codes are generated for each cell using the following code generation algorithm [18]

Generating iris code

{

For loop

{

MAX value=max (S1, S2, S3, S4);

MIN value=min (S1, S2, S3, S4);

If S (i) is located between MAX and MIN index

If S (i) is on the upward slope (iris pattern changes from darkness to brightness), set the cell's iris code to 1

If S (i) is on the downward slope (iris pattern changes from brightness to darkness), set the cell's iris code to 2 else set the cell's iris code to 0.

}

}

Each cell has two iris codes using the above algorithm; one for the horizontal group and the other for the vertical group.

3.4.2 Matching Stage using Hamming Distance

Once the iris codes are generated, the next stage is to measure the similarity between these iris templates using hamming distance classifier. Using the hamming distance, a decision can be taken as to whether the two templates belong to the same or different persons.

$$HD = \frac{1}{2N}[(\sum_{i=1}^{i=N} A_h(i) xor B_h(i)) + (\sum_{i=1}^{i=N} A_v(i) xor B_v(i))] \qquad (3.8)$$

where $A_h(i)$ and $A_v(i)$ are iris codes of the template 'A' in horizontal and vertical direction; and $B_h(i)$ and $B_v(i)$ are the iris codes of the new template in horizontal and vertical direction. N is the total number of the cells. The two iris templates belong to the same person if the hamming distance between them is very small and different persons if the hamming distance is large.

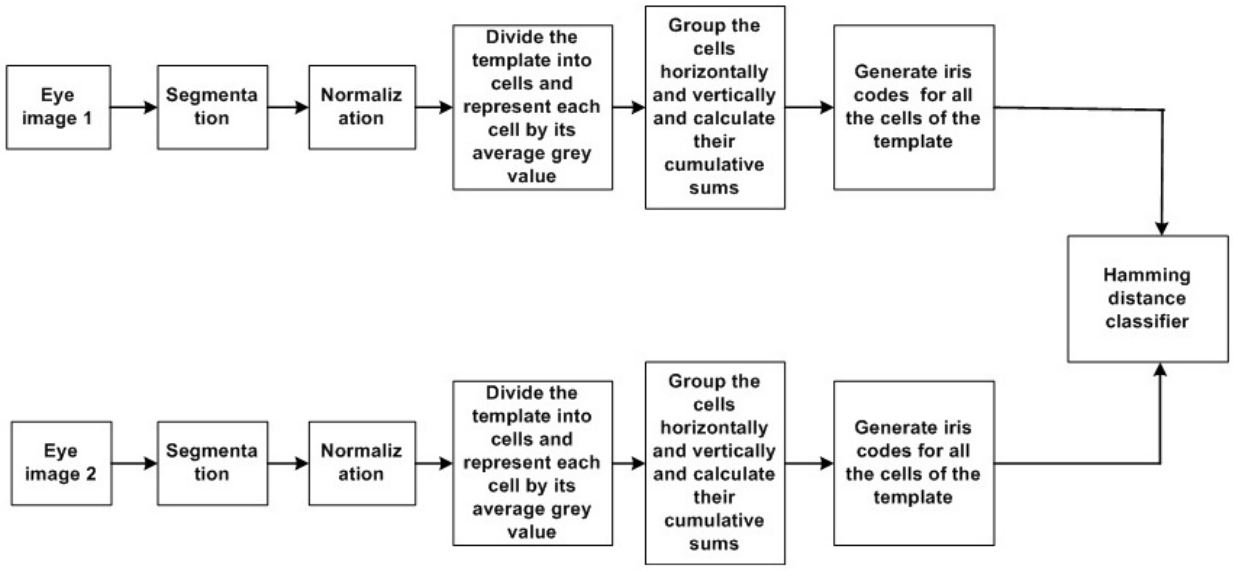

Figure 3.9 Block diagram of the iris recognition system using cumulative sum method

CHAPTER 4 - Experimental Results

4.1 Overview

In this report, methods for recognizing iris have been presented and their performances are evaluated. Tests were carried out using CASIA database and UBRIS.v1 database, to obtain the best separation hamming distance value, so that false accept rate (FAR) and false reject rate (FRR) are minimized and also to confirm that iris recognition system performs well as a biometric for recognizing individuals.

4.2 Data Set

The Chinese Academy of Sciences –Institute of Automation (CASIA) eye image data base [15] contains 756 grayscale images with 108 images of different persons or classes and 7 images of each person. These images were captured in two sessions with one month interval between sessions. These images were taken especially for iris recognition research developed by National Laboratory of Pattern Recognition, China. Features in the iris region are clearly visible due to the specialized imaging conditions.

UBRIS.v1 database [19] contains 1877 images with 241 images of different persons. These images were taken in two sessions during September 2004. These images were made available by Department of Computer Science, University of Beira Interior. To test the proposed algorithms, 90 eye images from the CASIA database and 30 eye images from UBRIS.v1 database are considered with three images for each person. So from the CASIA database the possible intra-class (same) comparisons are 90 and inter-class (different) comparisons are 3915. UBRIS.v1 database will result in 30 intra-class comparisons and 90 inter-class comparisons.

4.3 Experimental results of Method-1

In the proposed iris recognition method-1, 4-nearest neighbor classifier is used to classify the iris images, since we considered 3 images for each person. After computing feature vectors for the considered data set, Euclidean distance is computed from the test image vector to all the other feature vectors and the classes of the 4 nearest neighbors are taken into account. Some of the classifier outputs are shown in tables 4.1, 4.2, 4.3, 4.4. In the table 4.1, class 1 repeats twice

(maximum number of times). Therefore the test image belongs to the first person. In the table 4.2, class 2 repeats thrice. Therefore the test image belongs to the 2nd person. In the table 4.3, class 3 repeats thrice so, the test image belongs to the 3rd person. In the table 4.4, class 27 repeats thrice. Therefore the test image belongs to the 27th person. Among the 90 images of CASIA database, 64 images are recognized properly and using the UBRIS.v1 database 27 images is recognized properly. i.e., the nearest neighbors were of the same person as the test image. From the experimental results, the recognition performance of the proposed method is 71.11% with CASIA database and 88.8% with UBRIS.v1 database.

Simulation Results:

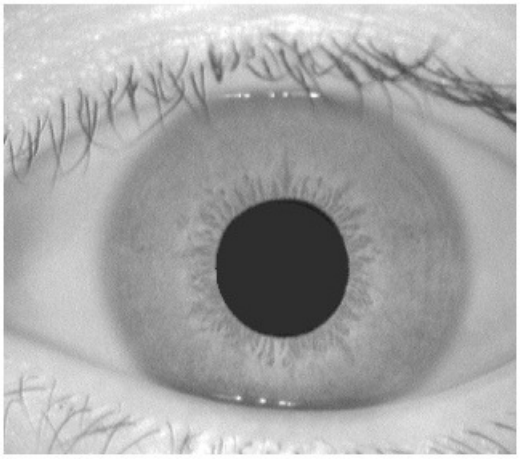

Figure 4.1 Original image of person-1

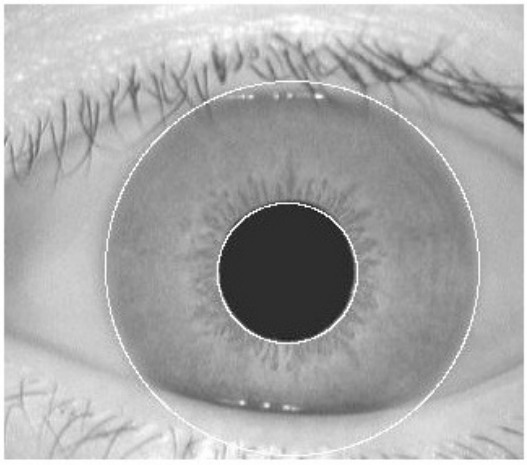

Figure 4.2 Segmented image of person-1

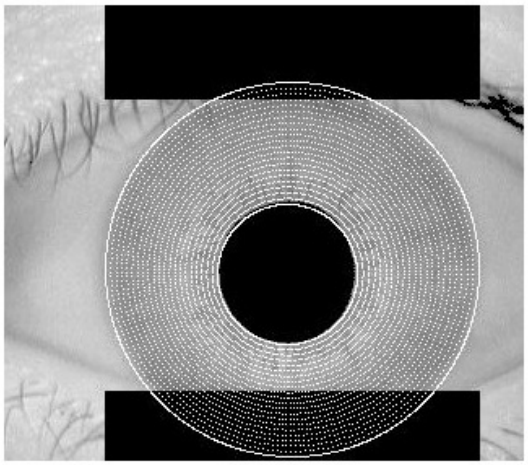

Figure 4.3 Normalized image of person-1

Figure 4.4 Extracted iris template

Figure 4.5 Template after applying Lifting Wavelet Transform

Classifier outputs of UBRIS.v1 database:

Distance	Class
0	1
0.4114	1
0.9450	8
1.0346	5

Table 4.1 Classifier output with person 1's third image as the test image

Distance	Class
0	2
0.4370	2
0.5389	2
0.6869	7

Table 4.2 Classifier output with person 2's first image as the test image

Distance	Class
0	3
0.1473	3
0.3918	3
0.6290	10

Table 4.3 Classifier output with person 3's first image as the test image

Classifier outputs of CASIA database:

Distance	Class
0	27
0.6990	27
0.7364	24
0.7547	27

Table 4.4 Classifier output with person 27's first image as the test image

Feature extraction is the crucial step to the success of an Iris recognition system. Feature extraction using multiresolution technique has proven high recognition accuracy in Daugman's method of Iris recognition system where Gabor filters were used to extract the phase information. To improve the performance of the proposed method-1, a combined multiresolution feature extraction scheme [17] of wavelet transform and Gabor filter bank can be used since Gabor filters with wavelet components provide useful information about texture features. Wavelet transforms allows us to detect the feature details efficiently and Gabor filters when applied on the wavelet components at different orientations improve the recognition accuracy.

4.4 False Acceptance Rate and False Rejection Rate

The main objective of an iris recognition system is to achieve a good separation hamming distance between intra-class (same) and inter-class (different) hamming distance distributions. The matching metric gives a range of hamming distance values when the templates generated from the same person's eye (intra-class comparisons) are compared, and another range of values when the templates are generated from different person's eye's (inter-class comparisons). By computing separation hamming distance, a decision can be taken as to whether the two iris templates belong to the same person or different persons. The intra-class and inter-class distributions generally overlap and result in false attempts and false rejects. Performance of the

proposed method is measured in terms of false accept rate (FAR) and false reject rate (FRR). False reject rate (FRR) measures the probability that an individual is not identified by the system [11]. It is also referred as Type 1 error [16]. False accept rate (FAR) measures the probability of an individual is wrongly identified as another individual [11]. FRR and FAR are calculated using the following equations. This is illustrated in the figure 4.6. In this figure, FRR is the area when the hamming distance of intra class distributions is greater than the set threshold and FAR is the area when the hamming distance of the inter class distributions is less than the set threshold.

$$FRR = \frac{\int_{i}^{1} P_{same}(x)dx}{\int_{0}^{1} P_{same}(x)dx} \tag{4.1}$$

$$FRR(\%) = \frac{number\ of\ \ false\ rejections}{Total\ number\ of\ \text{int}\ ra\ class\ comparisons} \tag{4.2}$$

$$FAR = \frac{\int_{0}^{i} P_{diff}(x)\,dx}{\int_{0}^{1} P_{diff}(x)dx} \tag{4.3}$$

$$FAR(\%) = \frac{number\ of\ \ false\ accep\ \tan ces}{Total\ number\ of\ \text{int}\ er\ class\ comparisons} \tag{4.4}$$

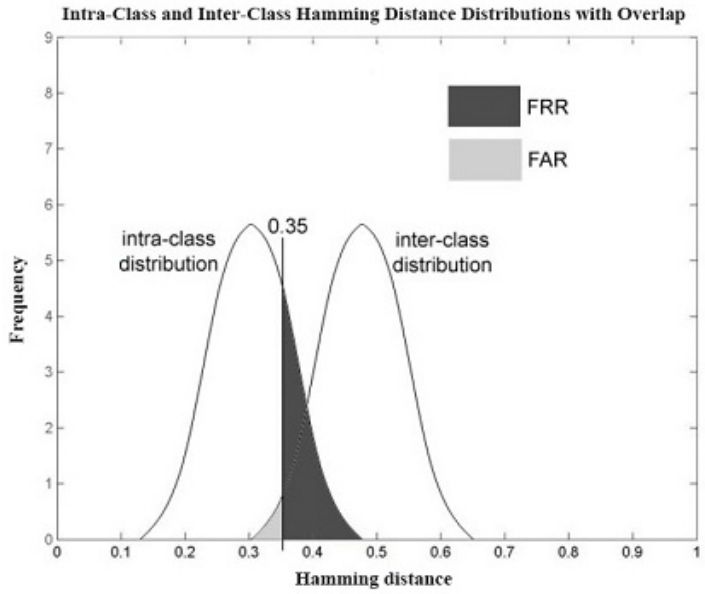

Figure 4.6 FRR and FAR curves with the separation hamming distance of 0.35 [11]

4.5 Experimental Results of Method-2

In this method, hamming distance classifier is used to measure the similarity between the templates. With 90 images, the possible intra-class (same) comparisons are 30 and inter-class (different) comparisons are 3915. Intra class distributions and the inter class distributions for the CASIA database are shown in the figure 4.7 and figure 4.8. The x-axis and y- axis indicate the hamming distance and number of samples (frequency) respectively. Intra class and inter class distributions are placed in the same plot as shown in the figure 4.9 to check whether the two distributions overlap or not. In this plot, hamming distance distributions slightly overlap. However the means of the intra and inter class distributions are separated, so recognition is possible. The recognition rate is determined by calculating the false accept and false reject rates with different separation points.

Figure 4.10 shows the FAR/FRR curves according to the hamming distance. False rejection rate is decreased when the hamming distance is increased and false acceptance rate is increased when the hamming distance value is increased respectively. So the two error curves have an intersection point. By selecting the intersection point of the two curves as a threshold, two error rates are minimized at the same time.

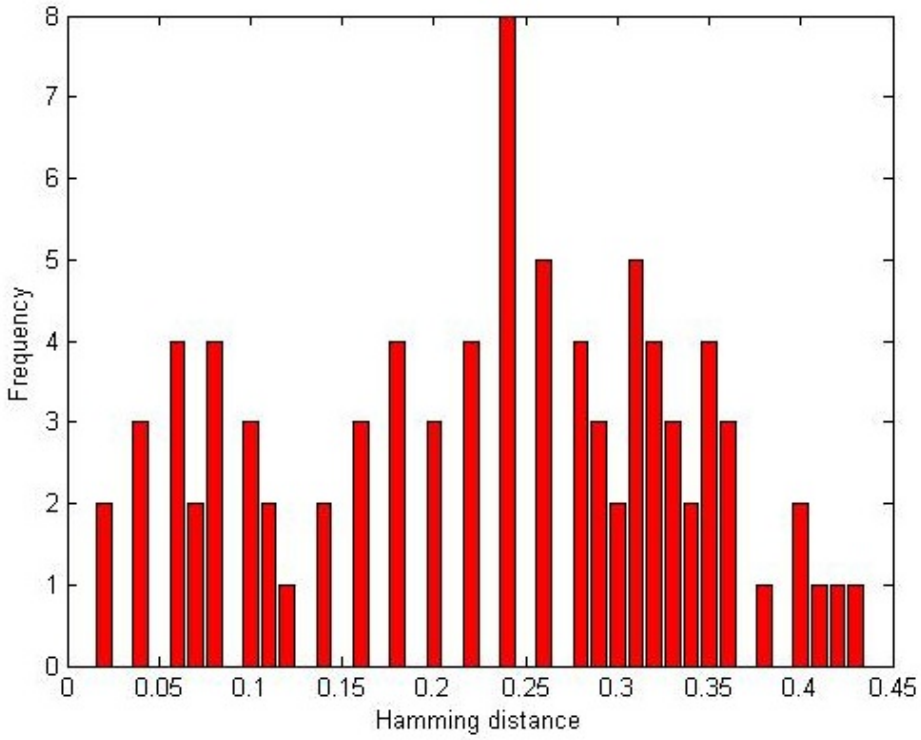

Figure 4.7 Intra- class distribution for CASIA dataset

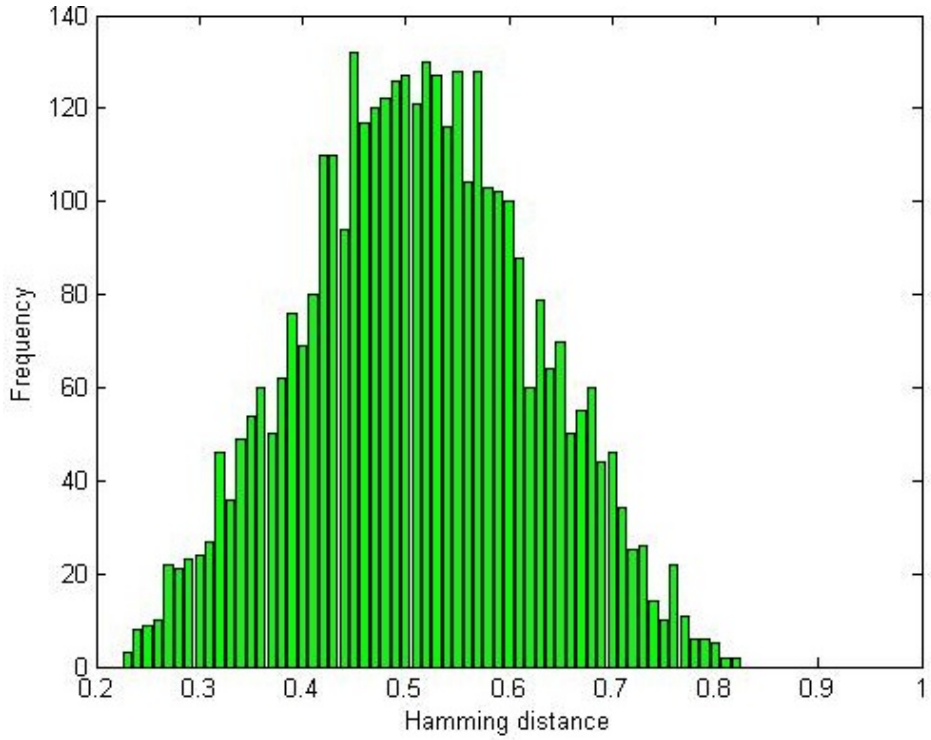

Figure 4.8 Inter-class distribution for the CASIA dataset

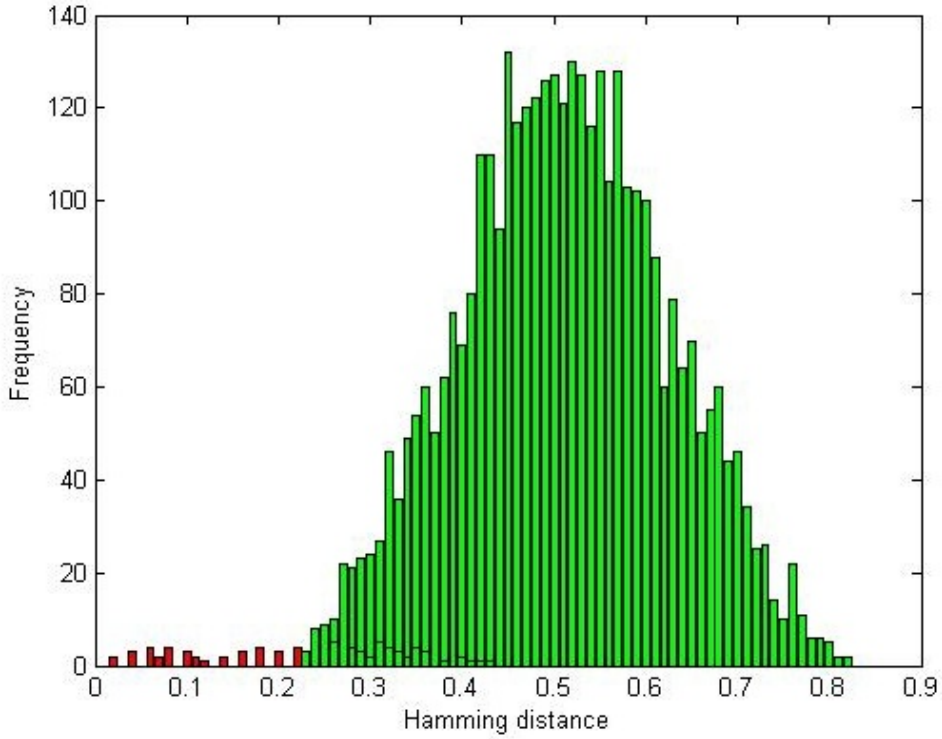

Figure 4.9 Intra and Inter class distributions for the CASIA dataset

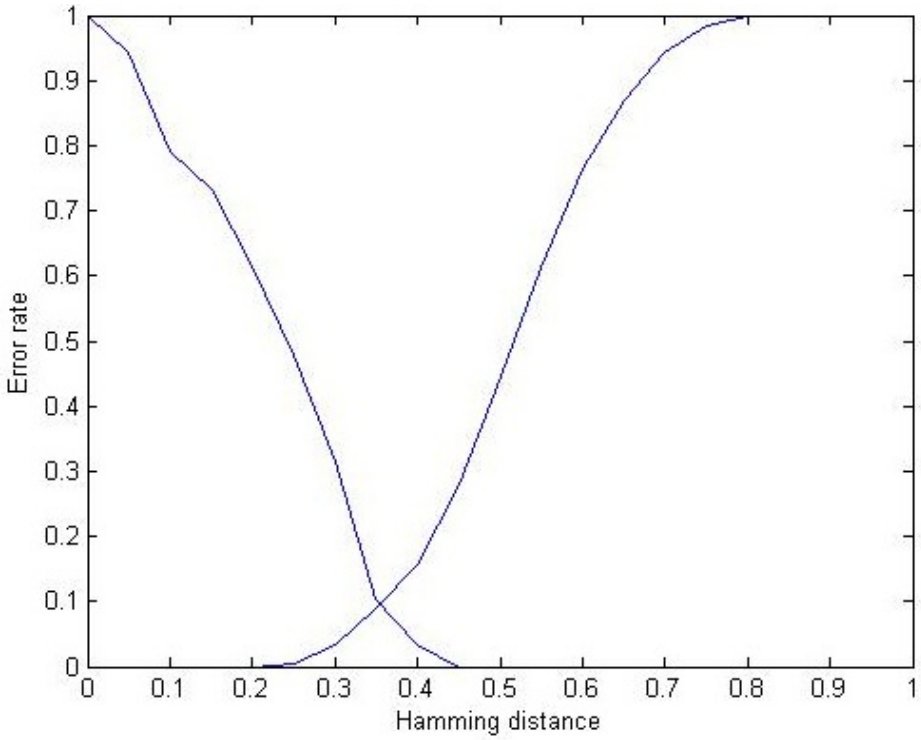

Figure 4.10 FRR and FAR curves for the CASIA dataset

Table 4.5 shows the FAR and FRR % according to the hamming distance. Recognition performance of the proposed method is 90.5% when the threshold is 0.35. The percentage of recognition will be more when the entire data base is considered. The experimental results show that the current method is an effective approach in iris recognition. With CASIA data set, perfect recognition is not possible due to the overlapping distributions. With the separation point of 0.35, a false accept rate and false reject rate of 0.085 and 0.095 is achieved.

Table 4.6 shows the recognition results of the current algorithms on CASIA database. We conclude that current method-2 shows the best performance. To improve the performance of the proposed method-1, a combined multiresolution feature extraction scheme [17] of wavelet maxima components and Gabor filter bank can be used since both, Gabor and wavelet transforms provide useful information about texture details.

Table 4.7 shows the feature execution times of the proposed two methods performed in Matlab 6.0. The proposed algorithms consume less time for extracting features. Feature extraction time for the proposed methods is calculated using the tic and toc commands in MATLAB.

Hamming distance	FAR%	FRR%
0.1	0%	82%
0.3	3.2%	28%
0.35	8.5%	9.5%
0.4	6%	15%

Table 4.5 FAR and FRR with different separation hamming distance values for the CASIA dataset

Methods	Recognition rate (%)
Proposed method-1 using wavelet transform	71.11%
Proposed method -2 using cumulative sum	90.50%

Table 4.6 Identification results on CASIA dataset

Methods	Feature Execution time
Proposed method-1 using wavelet transform	125.3 m sec
Proposed method-2 using cumulative sum	45.76 m sec

Table 4.7 Comparison of feature extraction times

CHAPTER 5 - Conclusion

5.1 Summary

This report presented two feature extraction methods for recognizing iris, which are tested using CASIA database, a database of digitized grayscale eye images. Iris images are extracted from the database using the segmentation and normalization algorithms mentioned in Libor Masek's thesis [11]. In this thesis, a segmentation algorithm is presented which localizes the iris region from an eye image and isolates eyelids, eyelashes. Segmentation is achieved using circular Hough transform for locating the iris and pupil regions, and linear Hough transform for detecting eyelids. Thresholding is employed for eliminating eyelashes. The segmented iris region is normalized and unwrapped into a rectangular block with fixed dimensions using Daugman's rubber sheet model.

Finally, features should be extracted from the unwrapped iris template. In the first feature extraction method, the iris template is divided into blocks and wavelet transform is applied to each block. Features are encoded by computing energy for each block of the iris template. Similarly, energy is computed for all the iris images. Based on the variance values, feature vectors are obtained for all the iris templates (training data and the test data). The training data (feature vectors of all the iris images) and the testing data (feature vector of the test image) are sent to the K-nearest neighbor classifier to recognize the iris images (find the nearest neighbors to the test data). The second method employs cumulative sum-based change analysis for extracting features. Here, a normalized iris image is divided into cells and codes are generated for these cells by the proposed code generation algorithm. Hamming distance is chosen as a classifier, which calculates the similarity between two iris codes. A lower hamming distance indicates higher similarity and the two templates were deemed to be generated from the same iris.

Analysis of the proposed iris recognition system has revealed numerous conclusions. Segmentation is the most critical stage of iris recognition system because data that is wrongly represented as iris pattern will corrupt the generated biometric template. With the CASIA database, 83% of the images are segmented properly. Among the two methods, the second

method gave a better recognition rate of 90.5% with the false accept and reject ratios of 0.085 and 0.095 respectively and also consumes less time for the feature extraction.

5.2 Suggestions for Future work

The methods presented in this report perform accurately. But there are few artifacts that need to be addressed. The automatic segmentation algorithm is not perfect, since it could not segment all the iris images of the database properly. Eyelashes were detected using thresholding technique in the proposed method and in some of the iris images, these eyelashes were included; they were not eliminated completely from the iris template. This problem is especially observed in persons with small eye and dense eyelashes. As a result, the segmentation accuracy is reduced. In order to improve the segmentation accuracy, a good eyelid and eyelash detection system should be implemented as the method suggested by W.K.Kong and D.Zhang [7].

In the normalization algorithm implemented by Daugman, only 20 data points are taken along the 240 radial lines that were drawn from the center of pupil. To improve the normalization algorithm, an even higher number of data points can be taken.

The performance of method-1 can be improved by using a combined multiresolution technique for feature extraction. A combination of Gabor filters and wavelet transform can be used for extracting features as the one suggested by Makram Nabti and Ahmed Bouridane [17]. The performance of method-2 can also be improved further by considering the size of the cell to be less than the one used.

The performance of the proposed iris recognition system can be improved by testing the algorithms with the more realistic data in various environments for making the iris recognition system more reliable. This system can be interfaced with an iris acquisition camera to capture number of images rather than working on iris image database. Video based recognition systems can be developed and used especially in the areas under surveillance to achieve high recognition rates without requiring the user to be in a controlled environment.

References

[1] J.Daugman, “How Iris Recognition works”, Proceedings of 2002 International Conference on Image Processing, Vol.1, 2002.

[2] J.Daugman, “High confidence visual recognition of persons by a test of statistical Independence”, IEEE Transaction. Pattern Analysis and Machine Intelligence, vol.15, 1993.

[3] J.Daugman, “Statistical richness of visual phase information: Update on recognizing persons by iris patterns,” International Journal on Computer Vision, vol.45, 2001.

[4] J.Daugman, “The importance of being random: Statistical principles of iris recognition,” Pattern Recognition, vol.36, 2003.

[5] R.P. Wildes, “Iris recognition: An emerging biometric technology,” Proceedings IEEE, vol.85, 1997.

[6] W.W.Boles and B. Boashash, “A human identification technique using images of the iris and wavelet transform,” IEEE Transactions on Signal Processing, vol. 46, 1998.

[7] W.K.Kong and D.Zhang, “Accurate iris segmentation based on novel reflection and eyelash detection model,” in Proceedings International Symposium Intelligent Multimedia, Video and Speech Processing, 2001.

[8] C.Tisse, L.Martin, L.Torres and M.Robert, “Person identification technique using human iris recognition,” in Proceedings 15th International Conference Vision Interface, 2002.

[9] S.Lim, K.Lee, O.Byeon and T.Kim, “Efficient iris recognition through improvement of feature vector and classifier,”ETRI Journal vol.23, 2001.

[10] Soumyadip Rakshit, Donald M. Monro “An evaluation of image sampling and Compression for human recognition,” in IEEE Transactions on Information Forensics and Security, vol.2, 2007.

[11] L.Masek, “Recognition of human iris patterns for biometric identification,” B.E. dissertation, Software Eng., Univ. Western Australia, Perth, Australia, 2003.

[12] L.Ma, T.Tan, Y.Wang and D.Zhang, “Efficient iris recognition by characterizing key local variations,” IEEE Transactions Image Processing, vol.13, 2004.

[13] John D. Woodward, Christopher Horn, Julius Gatune, and Aryn Thomas, “Biometrics, A look at facial recognition”, 2003.

[14] E.Wolff, “Anatomy of the Eye and Orbit”, 7th edition H.K.Lewis & Co.LTD, 1976.

[15] Chinese Academy of Sciences Institute of Automation (CASIA) database with 756 Grey scale Eye Images of 108 persons. Page http://www.sinobiometrics.com.

[16] J.Daugman, “Biometric decision landscapes”, Technical Report No. TR482, University of Cambridge Computer Laboratory, 2000.

[17] Makram Nabti, Ahmed Bouridane, “An effective and fast iris recognition system based on a combined multiscale feature extraction technique”.

[18] Jong-Gook Ko, Youn-Hee Gil, Jang-Hee Yoo, Kyo-IL Chung, “A Novel and Efficient Feature Extraction Method for Iris Recognition”.

[19] UBRIS.v1 database with 1877 digitized eye images of 241 persons.